# Magnetic self-field entry into a current-carrying type-II superconductor. II. Helical vortices in a longitudinal magnetic field

Yuri A. Genenko
*Donetsk Physico-Technical Institute of the Academy of Sciences of Ukraine, 340114 Donetsk, Ukraine*
(Received 9 June 1994)

The previous consideration of the irreversible magnetic self-field entry into a current-carrying type-II superconductor (SC) [Phys. Rev. B **49**, 6950 (1994)] is extended to the case of an applied longitudinal magnetic field. The structure of the helical Abrikosov vortex is found exactly in the framework of the London approximation. The field-dependent critical current of a spontaneous entry of the right-handed flux helix against the surface Bean-Livingston barrier into the SC cylinder of arbitrary radius $R$ is calculated, as well as the critical current of the flux-line instability with respect to the left-handed helical expansion. On the basis of these two mechanisms, a diagram of the resistive state in current-field coordinates is evaluated. The direction of the optimal helix for which the surface barrier is the least and which, hence, is the first to enter the sample turns out to coincide with that of the full magnetic field at the surface only in the case of a thick cylinder with $R \gg \lambda$, where $\lambda$ is the magnetic penetration depth. For the latter case, the generalized Silsbee's rule of a breakdown of nondissipative state is formulated.

## I. INTRODUCTION

A helical instability of flux lines (FL) and the flux-line lattice (FLL) is known to play a crucial role in the resistivity onset in current-carrying type-II superconductors (SC) in magnetic field parallel to current. The instability of individual FL's lying on the axis of a current-carrying SC cylinder with respect to expansion of helical perturbations was first considered by Clem.[1] The analogous instability of the longitudinal FLL against the growth of elliptical helical modes at sufficiently large currents was shown by Brandt.[2] These instabilities have close analogy to magnetohydrodynamic spiral instability, as was stressed in Ref. 1, and to the process of vortex ring nucleation,[3] referred to as the Onsager-Feynmann mechanism of viscosity onset in superfluids.

The origin of the above-mentioned instabilities is in driving forces exerted on the FL elements by the current density that make the left-handed spirals (or rings) expand. The same forces exerted on the right-handed spirals (or rings) make them contract resulting in an alternative mechanism of resistivity, namely, the irreversible entry of right-handed vortices (FL's) against the surface Bean-Livingston barrier and subsequent contraction due to both line tension and transport current driving force. The latter process was qualitatively considered in a lot of works (see in Ref. 4), but the critical currents and fields at which it should begin were not correctly established since it required the correct account of FL interaction with the specimen surface. As a matter of fact, the critical conditions of helical instability[1,2] cannot be correctly found either without a consistent account of surface influence. It is apparently significant both in thin samples[1] with transverse size of the order of $\lambda$, London penetration depth, and in the case of near-surface helical distortions of FLL.[2] Thus, the behavior of spiral FL's in a current-carrying type-II superconductor subjected to longitudinal magnetic field, including the possible interplay of left-handed helix expansion and right-handed helix entry resistive mechanisms, is not yet completely understood.

Recently a problem of vortex ring entry into a current-carrying SC cylinder was exactly solved in the framework of London approximation with regard to surface Bean-Livingston barrier.[5,6] In this paper we extend the analysis begun in Ref. 6 to the case including the magnetic field applied parallel to the cylinder and present the exact solution for the helical FL structure in the SC cylinder of an arbitrary radius. The Gibbs free energy of helical vortex evaluated with account of work done by sources of constant field and transport current enables us to find both critical currents for right-handed helical FL entry and left-handed helical FL instability. The two above mechanisms acting in a pin-free ideal SC sample define the diagram of resistive state in the current-field coordinates ($j$-$H$).

## II. STRUCTURE OF A HELICAL MAGNETIC VORTEX IN SUPERCONDUCTING CYLINDER

A helical magnetic vortex inside the SC specimen may be described by means of the Maxwell equation and London equation[4] with a special right-hand side (rhs) $\Phi$:

$$\begin{aligned} &\mathrm{div}\mathbf{h}=0\ , \\ &\lambda^2\mathrm{curl}\,\mathrm{curl}\mathbf{h}+\mathbf{h}=\mathbf{\Phi}\ , \end{aligned} \tag{1}$$

where

$$\mathbf{\Phi}=\Phi_0\frac{\mathbf{e}_1}{\mathbf{e}_1\mathbf{e}_\varphi}\delta(\rho-r)\delta(z-L\varphi)$$

is presented in cylindrical coordinates $(\rho,\varphi,z)$ with the $z$ axis coinciding with the axis of a cylindrical sample of radius $R$; $\mathbf{e}_\varphi$ the unit azimuthal vector: $\mathbf{e}_1$ the unit vector tangential to helical core of the vortex, lying on the imaginary cylinder of the radius $r$; and $2\pi L$ the pitch length of

 

the spiral vortex. The above choice of $\Phi$ provides that the flux of magnetic field $\mathbf{h}$ through any plane crossing the helix only one time $\int \mathbf{h} d\mathbf{s} = \Phi_0$ (in the infinite bulk, i.e., at $R \to \infty$). Let us note that $\Phi$ also satisfies the requirement $\mathrm{div}\Phi = 0$ for the London equation to be consistent with the Maxwell one.

Outside the cylinder the magnetic field is described by Maxwell equations in empty space

$$\begin{aligned} &\mathrm{div}\mathbf{h} = 0 , \\ &\mathrm{curl}\mathbf{h} = 0 . \end{aligned} \tag{2}$$

The boundary conditions for Eqs. (1) and (2) follow from the requirements of continuity of the field at the SC cylinder boundary ($\rho = R$) and vanishing of the field at the infinity ($\rho \to \infty$).[7]

Being presented in cylindrical components $h = (h_\rho, h_\varphi, h_z)$ the London equation (1) reads

$$\Delta h_\rho - \left[\frac{1}{\rho^2} + \frac{1}{\lambda^2}\right] h_\rho - \frac{2}{\rho^2}\frac{\partial h_\varphi}{\partial \varphi} = 0 , \tag{3}$$

$$\Delta h_\varphi - \left[\frac{1}{\rho^2} + \frac{1}{\lambda^2}\right] h_\varphi + \frac{2}{\rho^2}\frac{\partial h_\rho}{\partial \varphi} = -\frac{\Phi_0}{\lambda^2}\delta(\rho - r)\delta(z - L\varphi) , \tag{4}$$

$$\Delta h_z - \frac{1}{\lambda^2} h_z = -\frac{\Phi_0}{\lambda^2}\frac{L}{r}\delta(\rho - r)\delta(z - L\varphi) , \tag{5}$$

where the Laplace operator in cylindrical coordinates is

$$\Delta Y = \frac{1}{\rho}\frac{\partial}{\partial \rho}(\rho Y) + \frac{1}{\rho^2}\frac{\partial^2 Y}{\partial \varphi^2} + \frac{\partial^2 Y}{\partial z^2} .$$

To simplify the problem let us note two points. First is that the magnetic field is potential outside the SC specimen that enables one to present it by means of some scalar potential $\psi$ as $H = \nabla\psi$. The latter satisfies the Poisson equation

$$\Delta\psi = 0 \tag{6}$$

following from Eqs. (2). The second point is that the helical symmetry of the problem allows one to express the dependencies on $z$ and $\varphi$ variables as functions of one variable $\zeta$: $L\zeta = z - L\varphi$. Clearly, the field components are periodical in $\zeta$ with a period of $2\pi$ and, thus, may be presented by Fourier series as

$$\begin{aligned} h_\rho(\rho,\zeta) &= \sum_k e^{ik\zeta} a_k(\rho) , \\ h_\varphi(\rho,\zeta) &= \sum_k e^{ik\zeta} b_k(\rho) , \\ h_z(\rho,\zeta) &= \sum_k e^{ik\zeta} c_k(\rho) \\ \psi(\rho,\zeta) &= \sum_k e^{ik\zeta} \psi_k(\rho) . \end{aligned}$$

Finally, the full set of equations in Fourier amplitudes acquires the form

$$\frac{\partial^2 a_k}{\partial \rho^2} + \frac{1}{\rho}\frac{\partial a_k}{\partial \rho} - \frac{1+k^2}{\rho^2} a_k - \left[\frac{1}{\lambda^2} + \frac{k^2}{L^2}\right] a_k + i\frac{2k}{\rho^2} b_k = 0 , \tag{7}$$

$$\frac{\partial^2 b_k}{\partial \rho^2} + \frac{1}{\rho}\frac{\partial b_k}{\partial \rho} - \frac{1+k^2}{\rho^2} b_k - \left[\frac{1}{\lambda^2} + \frac{k^2}{L^2}\right] b_k - i\frac{2k}{\rho^2} a_k = -\frac{\Phi_0}{2\pi\lambda^2 L}\delta(\rho - r) , \tag{8}$$

$$\frac{\partial^2 c_k}{\partial \rho^2} + \frac{1}{\rho}\frac{\partial c_k}{\partial \rho} - \frac{k^2}{\rho^2} c_k - \left[\frac{1}{\lambda^2} + \frac{k^2}{L^2}\right] c_k = -\frac{\Phi_0}{2\pi\lambda^2 r}\delta(\rho - r) , \tag{9}$$

$$\frac{\partial^2 \psi_k}{\partial \rho^2} + \frac{1}{\rho}\frac{\partial \psi_k}{\partial \rho} - \frac{k^2}{\rho^2}\psi_k - \frac{k^2}{L^2}\psi_k = 0 , \tag{10}$$

with boundary conditions

$$\begin{aligned} a_k(R) &= \frac{\partial \psi_k}{\partial \rho}(R) , \\ b_k(R) &= \frac{-ik}{R}\psi_k(R) , \\ c_k(R) &= \frac{ik}{L}\psi_k(R) , \\ \psi_k(\infty) &= 0 . \end{aligned} \tag{11}$$

Equations (9) and (10) part from the set of Eqs. (7)–(10) and may be solved separately in terms of the modified Bessel functions $I_k(x)$ and $K_k(x)$.[8] The account of boundary conditions (11) and the requirement that $\mathbf{H}$ be finite at $\rho = 0$ and vanish at $\rho \to \infty$ lead to the following solutions:

$$\psi_k(\rho) = d_k K_k(|k|\rho/L) , \tag{12}$$

$$c_k = \frac{\Phi_0}{2\pi\lambda^2}\left[\vartheta(\rho - r) P_k^k(r,\rho) + \vartheta(r - \rho) P_k^k(\rho, r)\right] + \frac{ikd_k}{L}\frac{I_k(\kappa_k \rho/r)}{I_k(\kappa_k)} K_k\left[\frac{|k|R}{L}\right] , \tag{13}$$

where the notations $\kappa_k^2 = (R/\lambda)^2 + k^2(R/L)^2$ and

$$P_l^k(x,y) = [I_l(\kappa_k) K_l(\kappa_k y/R) - I_l(\kappa_k y/R) K_l(\kappa_k)] \times \frac{I_l(\kappa_k x/R)}{I_l(\kappa_k)}$$

are introduced. The unknown coefficients $d_k$ will be found below.

Consider the coupled equations [(7) and (8)]. They may be separated from each other by introducing the complex amplitudes $f_k^\pm = a_k \pm i b_k$ which satisfy the equation

$$\frac{\partial^2 f_k^\pm}{\partial \rho^2} + \frac{1}{\rho}\frac{\partial f_k^\pm}{\partial \rho} - \frac{(1 \mp k)^2}{\rho^2} f_k^\pm - \left[\frac{1}{\lambda^2} + \frac{k^2}{L^2}\right] f_k^\pm = \mp\frac{i\Phi_0}{2\pi\lambda^2 L}\delta(\rho - r) \tag{14}$$

following from Eqs. (7) and (8). The latter equation may be easily solved,[8] and then the solutions of Eqs. (7) and (8) satisfying the boundary condition (11) and requirement that field be finite at $\rho=0$ read

$$\begin{Bmatrix} a_k \\ ib_k \end{Bmatrix} = \frac{i\Phi_0 r}{4\pi\lambda^2 L}[\vartheta(r-\rho)[P^k_{k-1}(\rho,r)\mp P^k_{k+1}(\rho,r)]+\vartheta(\rho-r)[P^k_{k-1}(r,\rho)\mp P^k_{k+1}(r,\rho)]] - d_k\frac{|k|}{2L}\left[\frac{I_{k-1}(\kappa_k\rho/R)}{I_{k-1}(\kappa_k)}K_{k-1}\left[\frac{|k|R}{L}\right]\pm\frac{I_{k+1}(\kappa_k\rho/R)}{I_{k+1}(\kappa_k)}K_{k+1}\left[\frac{|k|R}{L}\right]\right] . \tag{15}$$

To obtain the coefficients $d_k$ one can use the Maxwell equation of Eqs. (1) inside the SC sample that, in Fourier components, takes the form

$$\frac{\partial a_k}{\partial\rho}+\frac{a_k}{\rho}-\frac{ikb_k}{\rho}+\frac{ik}{L}c_k=0 . \tag{16}$$

Then

$$d_k=\frac{i\Phi_0 r}{2\pi\lambda^2|k|}\frac{[I_{k+1}(\kappa_k r/R)/I_{k+1}(\kappa_k)-I_{k-1}(\kappa_k r/R)/I_{k-1}(\kappa_k)]}{\kappa_k I_k(\kappa_k)[K_{k-1}(|k|R/L)/I_{k-1}(\kappa_k)+K_{k+1}(|k|R/L)/I_{k+1}(\kappa_k)]+2|k|(R/L)K_k(|k|R/L)} . \tag{17}$$

One can see that $c_k$ and $b_k$ are even in the subindex $k$ while $a_k$ and $d_k$ are odd, particularly $a_0=d_0=0$.

Equations (12), (13), (15), and (17) provide the full description of the helical vortex. In the case of the zero twist (when the pitch length $L\to\infty$) $h_\rho$ and $h_\varphi$ vanish as $1/L$ together with $a_k$ and $b_k$ (15) while $h_z$ transforms to the well-known solution for the longitudinal linear vortex in a SC cylinder (see, for example, in Ref. 9). Let us note that the limit of the set of vortex rings[6] cannot be reached at $L\to 0$ starting from the solution (12)–(17) because helical and ring flux configurations are topologically different.

Really, the magnetic flux flowing through the helical vortex in $z$ direction is

$$\Phi_z(r)=\int_0^{2\pi}d\varphi\int_0^R d\rho\,\rho h_z(\rho,\zeta) =2\pi\int_0^R d\rho\,\rho c_0(\rho)=\Phi_0[1-I_0(r/\lambda)/I_0(R/\lambda)] \tag{18}$$

at any $L$, while this quantity for vortex ring equals zero.[6] The flux flowing through the vortex in the azimuthal direction equals

$$\Phi_\perp=\int_0^\infty d\rho\int_z^{z+2\pi L}dz\,h_\varphi(\rho,\zeta) =2\pi L\int_0^\infty d\rho b_0(\rho)=\Phi_0\left\{1-\frac{r}{\lambda}K_1\left[\frac{r}{\lambda}\right]-\frac{r}{R}\frac{I_1(r/\lambda)}{I_1(R/\lambda)}\left[1-\frac{R}{\lambda}K_1\left[\frac{R}{\lambda}\right]\right]\right\} \tag{19}$$

which, in the infinite bulk case ($R\to\infty$), gives the value

$$\Phi_\perp(\infty)=\Phi_0[1-(r/\lambda)K_1(r/\lambda)]$$

that coincides with that of vortex ring in the bulk.[10]

## III. GIBBS FREE ENERGY OF A CYLINDER WITH A HELICAL VORTEX

To study the problem of an energy barrier against the helical magnetic vortex entry into the current-carrying superconductor or the problem of instable vortex exit out of specimen one should evaluate the change in the Gibbs free energy of the system, $\Delta G$, arising due to the vortex motion when an external magnetic field and transport current are applied. The quantity $\Delta G$ may be calculated, as in the spirit of Ref. 11, as

$$G=F-\Delta W_I-\Delta W_H , \tag{20}$$

where $F$ is the self-energy contribution, $\Delta W_I$ is the work done by the source of transport current $I$, and $\Delta W_H$ is the work done by the source of external magnetic field $H$.

The position-dependent self-energy contribution to the free energy may be found using the conventional definition[4,12]

$$F=\frac{1}{8\pi}\int_{\rho\le R}[\mathbf{h}^2+\lambda^2(\mathrm{curl}\mathbf{h})^2]dV+\frac{1}{8\pi}\int_{\rho>R}\mathbf{h}^2dV \tag{21}$$

with the help of the vector identity

$$(\mathrm{curl}\mathbf{h})^2=\mathbf{h}\,\mathrm{curl}[\mathrm{curl}(\mathbf{h})]+\mathrm{div}[\mathbf{h}\times\mathrm{curl}(\mathbf{h})] .$$

Finally (see Appendix A),

$$F=\frac{1}{8\pi}\int dV\mathbf{h}\Phi =\frac{\Phi_0}{8\pi}\left[h_z(\rho=r,0)+\frac{r}{L}h_\varphi(\rho=r,0)\right] . \tag{22}$$

Although strictly speaking the field components diverge logarithmically at the vortex core in the London approximation, the actual field saturates at $\rho=r$ within the scale of $\xi$, SC correlation length.[12] Hence, the values of field components in the rhs of Eq. (22) may be evaluated as

$$h_\varphi(r,0)=\sum_k b_k(r-\xi),\quad h_z(r,0)=\sum_k c_k(r-\xi) .$$

Approximate calculation of the free energy by summation of the above expressions yields, for a wide range of $r$ except for $r \ll R, \lambda, L$,

$$F=\left[\frac{\Phi_0}{4\pi\lambda}\right]^2\left\{\frac{I_0(r/\lambda)}{I_0(R/\lambda)}[I_0(R/\lambda)K_0(r/\lambda)-I_0(r/\lambda)K_0(R/\lambda)]\right.$$
$$+\left[\frac{r}{L}\right]^2\frac{I_1(r/\lambda)}{I_1(R/\lambda)}[I_1(R/\lambda)K_1(r/\lambda)-I_1(r/\lambda)K_1(R/\lambda)]$$
$$\left.+\sqrt{1+r^2/L^2}\ln\left[\frac{1-\exp\{2[\varphi(r/L)-\varphi(R/L)]\}}{(\xi/L)[L/r+(r/L)(1+\sqrt{1+r^2/L^2})^{-1}]}\right]\right\}, \tag{23}$$

where $\varphi(x)=\sqrt{1+x^2}-\ln(1/x+\sqrt{1+1/x^2})$. This approximation is quite valid for the vortex entry problem. For the helical instability problem, though, it is the small-$r$ region that is essential. The latter will be studied in the next section. The details of the free-energy calculation are presented in Appendix B.

In a cylinder configuration, the external field work (per unit length along the $z$ axis) may be simply found as

$$\Delta W_H=\frac{1}{4\pi}\int \mathbf{hH}\,dV=H\Phi_z(r)/4\pi\ , \tag{24}$$

where $\Phi_z(r)$ was already obtained in Eq. (18).

To find the work done by the source of the transport current as the vortex is introduced, $\Delta W_I$, let us note that final result must be independent of the position of the conductor returning to the source of the current $I$, which is supplied to the specimen. Let us compute $\Delta W_I$ by supposing that the return conductor has coordinates $(x,y)=(-\infty,0)$ as is schematically shown in Fig. 1.

When the helical FL moves toward the cylinder axis, the flux $\Phi'$ flowing upward through a source circuit (shown in Fig. 1 by a dashed line) changes with time, producing a back emf of $E_i=-(1/c)(d\Phi'/dt)$. Then the source of the current $I$ will have to provide the emf of the same magnitude but opposite sign, $E'=-E_i$, in order to maintain the current $I$ constant.[11]

This process in our geometry seems a bit complicated for when the flux $\Phi'$, consisting of the array of flux spots, enters from the left edge of a cylinder moving to the right, from another edge of the cylinder the magnetic flux of the same magnitude but of opposite sign, $\Phi''=-\Phi'$, moves to the left, as is shown in Fig. 1. Using the scheme proposed in Ref. 6, one can circumvent the difficulty as follows.

Imagine the cylinder to be divided in two equal parts and present the source circuit in the equivalent form shown in Fig. 1(a). Then the work done by the source of current is

$$\Delta W_I=\int dt(E'I_1+E''I_2)\ , \tag{25}$$

where the two terms in the integrand stand for the work done in the two branches of equivalent circuit, $I_1$ and $I_2$ are the currents flowing in the left and right branches of the circuit, respectively, and integration is carried out over the time of vortex motion from the edge of the cylinder to the position with some radius $r$. In the above expression $E'=c^{-1}d\Phi'/dt$ is the emf applied to the left conductor by the source of the current when magnetic flux $\Phi'$ leaves the contour shown in Fig. 1 by a dashed line, crossing the left edge of the cylinder, and $E''=c^{-1}d\Phi''/dt$ is the emf arising in the right branch of the circuit when the flux $\Phi''$ enters the right edge of the cylinder. Since $\Phi''=-\Phi'$ and moves in a direction oppo-

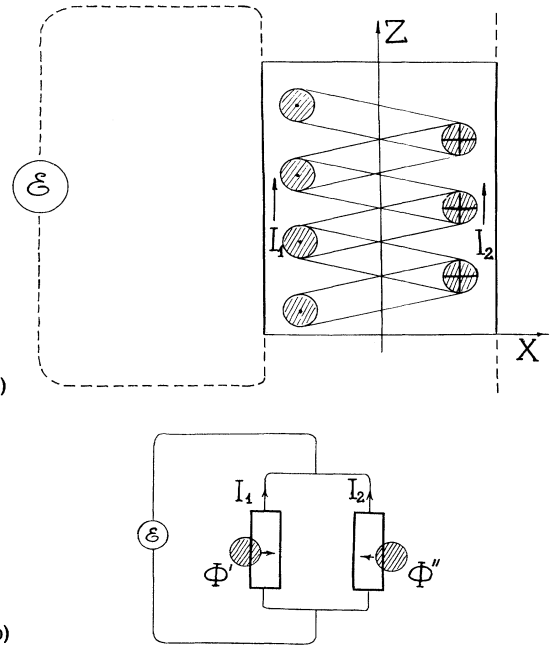


FIG. 1. (a) Schematic view of magnetic helical vortex inside the infinitely long superconducting cylinder with axis $z$. The spiral vortex core lies on the cylinder of radius $r$ and has a pitch length of $2\pi L$. The current source circuit is indicated by a dashed line. The conductor returning back to the current source has coordinates $(x,y)=(-\infty,0)$. The transport current $I$ as well as external magnetic field $H$ are in the positive direction of the $z$ axis. The array of dashed spots shows the cross sections of the spiral magnetic flux by the $x$-$z$ plane. (b) Sketches of the equivalent circuit obtained by imaginary division of the cylinder into two symmetrical parts. $\Phi'$ measures the magnetic flux leaving the source circuit by entering the left edge of cylinder $x=-R$. $\Phi''=-\Phi'$ is the flux entering simultaneously the right edge of the cylinder $x=R$ from outside. $I_1$ and $I_2$ are the currents flowing in the branches of equivalent circuit.

site to that of $\Phi'$, it is obvious that $E'=E''$. Taking into account that $I_1+I_2=I$, one gets

$$\Delta W_I=\int E'Idt=\frac{1}{c}I\Phi_I(r)\ , \tag{26}$$

where the quantity $\Phi_I(r)$ measures the magnetic flux leaving the source circuit when the helical vortex moves from the edge of the cylinder to a position with radius $r$. The latter formula reduces the problem of finding the Gibbs free energy to finding the magnetic flux leaving the source circuit in the course of vortex motion.

The value of $\Phi_I(r)$ can be defined as the change in the total magnetic flux flowing through the source circuit. The latter is equal to the integral of the magnetic field over the left half-plane

$$\Phi_t(r)=\int_{-\infty}^{-R}dx\int_{-\infty}^{+\infty}dz\,|h_\varphi(\rho,z)|=\oint \mathbf{A}d\mathbf{l}\ , \tag{27}$$

where the $\mathbf{A}$ is vector potential connected to $\mathbf{h}$ by definition $\mathbf{h}=\mathrm{curl}\,\mathbf{A}$. The integration of the rhs of (27) is over the path shown by the dashed line in Fig. 1.

As we are interested in the change of $\Phi_t$ only, the infinite constant contribution to the integral (27) from the transport current field may be omitted. Then one can substitute into (27) the vector potential induced by the vortex presence only. The vector potential $\mathbf{A}$ is connected to the current $\mathbf{j}$ by a generalized London equation:[12,13]

$$\mathbf{j}=\frac{c}{4\pi\lambda^2}(\mathbf{S}-\mathbf{A})\ , \tag{28}$$

where $\mathbf{S}$ is a source function defined in such a way that $\mathrm{curl}\mathbf{S}=\mathbf{\Phi}$. Taking into account that $\mathbf{A}$ vanishes as $\rho$ goes to infinity, the path of integration in (27) reduces to the left edge of cylinder $x=-R$. The $\mathbf{S}$ function in (28) does not contribute to the integral in (27) since the corresponding $\delta$ function on the rhs of Eq. (1) is centered beyond the contour of integration. Finally, one finds

$$\Phi_t(r)=-\frac{4\pi\lambda^2}{c}\int_{-\infty}^{+\infty}dz\,j_z(\rho=R,z)\ . \tag{29}$$

Taking into account that, in cylindrical coordinates,

$$j_z(R,z)=\frac{c}{4\pi R}\left[\frac{\partial}{\partial\rho}(\rho h_\varphi)-\frac{\partial h_\rho}{\partial\varphi}\right]$$

$$=\frac{c}{4\pi R}\sum_k\left[\frac{\partial}{\partial\rho}(\rho b_k)+ika_k\right]e^{ikz}\ , \tag{30}$$

one obtains the $\Phi_t(r)$ value per unit length along the $z$ axis:

$$\Phi_t'(r)=-\frac{\lambda^2}{R}\frac{\partial}{\partial\rho}[\rho b_0(\rho)]$$

$$=\frac{\Phi_0}{2\pi L}\frac{r}{R}I_1(\kappa_1 r/R)/I_1(\kappa_1)\ . \tag{31}$$

Then the quantity of interest $\Phi_I(r)=\Phi_t'(R)-\Phi_t'(r)$ that yields

$$\Phi_I(r)=\frac{\Phi_0}{2\pi L}\left[1-\frac{rI_1(r/\lambda)}{RI_1(R/\lambda)}\right]\ . \tag{32}$$

Note that the change in $\Phi_z$ or $\Phi_\perp$ after the helix motion from the edge of cylinder to the final position on the $z$ axis does not equal $\Phi_0$. Nevertheless, the flux leaving the source circuit during this process, $\Phi_I(0)$, equals $\Phi_0$. Thus, the entry of a single FL into the cylinder means, at any $R$ and $L$, an escape of strictly one flux quantum from the contour shown by the dashed line in Fig. 1. One can also see that the quantities $\Phi_I(r)$ and $\Phi_\perp$ are quite different.

Finally, the Gibbs free energy, resulting from the above consideration is

$$G=F-\frac{H\Phi_0}{4\pi}\left[1-\frac{I_0(r/\lambda)}{I_0(R/\lambda)}\right]$$

$$\pm\frac{I\Phi_0}{2\pi cL}\left[1-\frac{rI_1(r/\lambda)}{RI_1(R/\lambda)}\right]\ , \tag{33}$$

where the upper sign corresponds to the left-handed and the lower sign to the right-handed helices.

## IV. CRITICAL CURRENT OF A HELIX ENTRY AGAINST A SURFACE BARRIER

The dependence of $G$ on spiral vortex radius $r$ exhibits the edge barrier for vortex entry for any fixed $L$ (see Fig. 2). The barrier width and height depend on the current and field applied. When the current $I$ (or, alternatively, field $H$) exceeds some field-dependent critical value $I_c(H)$ [respectively, $H_c(I)$] the barrier vanishes and spontaneous nucleation of helical vortex on the surface occurs.

One can estimate the critical parameters for spontaneous entry of a vortex, using the criterion $\partial G/\partial r|_{r\to R}=0$, corresponding to the vanishing of the edge barrier. Because of the logarithmic divergency of free energy (23) at the edge of the cylinder (where the vortex merges with its image) the derivative should be taken at $r=R-\xi/2$, where the free energy (23) vanishes.

In the vicinity of the cylinder surface $R-r\ll R$, $\lambda$, the free energy (23) takes a simple form

$$F=(\Phi_0/4\pi\lambda)^2\sqrt{1+s^2}\ln[2(R-r)/\xi]\ , \tag{34}$$

where $s=R/L$ stands for the tangent of the tilt angle $\alpha$ of the helix to the $z$ axis. Substituting formula (34) into

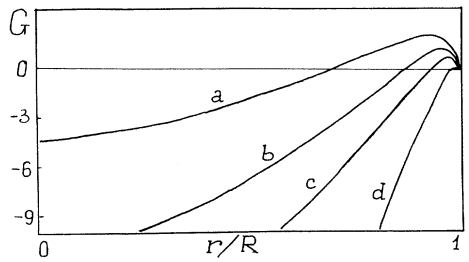


FIG. 2. The Gibbs free energy per unit length [in units of $(\Phi_0/\lambda)^2$] of the SC cylinder of radius $R=0.5\lambda$ containing the right-handed helical magnetic vortex with pitch length $L=0.5\lambda$, against the helix radius $r$. The applied parallel magnetic field $H=H_C$. Transport current density is $j/j_L=0$ ($a$), 0.2 ($b$), 0.4 ($c$), 0.97 ($d$).

Eq. (33) and making use of the above-stated criterion, one can find the value of a critical field

$$h_{cr}(j,s)=H_c[I_0(R/\lambda)/I_1(R/\lambda)](\sqrt{1+s^2}-sj/j_L)\ , \tag{35}$$

depending on the current density on the sample surface $j$ and $s$, where $H_c=\Phi_0/2\sqrt{2}\pi\lambda\xi$ is the thermodynamical critical field and $j_L=cH_c/4\pi\lambda$ is the London value for critical current density.

This dependence has a minimum in $s$ that enables one to find an optimal helix for which the least critical current (or critical field) of entry is achieved and which, hence, first enters the sample. Minimizing $h_{cr}(j,s)$ with respect to $s$ one finds the optimal helix pitch length

$$L=R\sqrt{(j_L/j)^2-1}\ . \tag{36}$$

Then, upon substitution of the length (36) into Eq. (35), one can see that the corresponding values of the critical current $j_{cr}$ and field $H_{cr}$ for the optimal helix entry satisfy a simple equation

$$(I_1(R/\lambda)/I_0(R/\lambda))^2(H_{cr}/H_c)^2+(j_{cr}/j_L)^2=1 \tag{37}$$

that describes a ringlike nondissipative region in the coordinates current-field ($j$-$\eta$).

The tilt of the optimal vortex to the $z$ axis following from Eqs. (36) and (37) equals

$$tg\alpha=R/L=\nu^{-1}(j/j_L)/(H/H_c)\ ,$$

where the size-dependent number $\nu$ stands for $I_1(R/\lambda)/I_0(R/\lambda)$. At the same time the tilt of the full magnetic field lines at the surface $H_I/H=\nu(j/j_L)/(H/H_c)$, where we used the transport current distribution over the cross section of the SC cylinder

$$j(r)=(I/2\pi R\lambda)I_0(R/\lambda)/I_1(R/\lambda)$$

and the value of a current self-field at the surface $H_I=2I/cR$. One can see that, $tg\alpha$ coincides with $H_I/H$ only for thick samples with $R\gg\lambda$ when $\nu\to 1$.

The latter notations allows one to rewrite Eq. (37) in a rather clear form:

$$(\nu H)^2+(H_I/\nu)^2=H_c^2\ . \tag{38}$$

Taking into account that, for $R\gg\lambda$, the terms on the left-hand side form simply the squared full field at the surface, one can see that, for the case of parallel field applied, the *generalized Silsbee's rule*[14] for thick samples with ideal surface (with surface defect size $\delta\ll\lambda\ll R$) turns out to be valid in the following form: In a thick ideal current-carrying superconductor, subjected to a longitudinal magnetic field, the breakdown of the nondissipative state occurs when the full magnetic field at the surface first attains the magnitude of the thermodynamic critical field $H_c$.

It is easy to see that at low fields the critical current of the helix entry achieves the value of $j_L$ for an ideal surface case coinciding with that of vortex ring entry. Though the value $j_L$ is very high and achieves a magnitude of $10^9$ A/cm$^2$, it seems to have been observed in experiments of HTSC microbridges as was reported in Ref. 15. At low current the critical field of helix entry tends to that of straight-line vortex.[9] The account of the possibility of vortex entry on the surface defects may, generally speaking, decrease the critical parameters in the thick sample case with $R\gg\lambda$ (Ref. 6) that will be discussed below in Sec. VI.

## V. SPIRAL INSTABILITY OF A HELICAL VORTEX IN A LONGITUDINAL FIELD

As was shown in a previous section, when the current density on the SC sample surface exceeds the critical value $j_{cr}(H)$, the spontaneous entry of helical vortices against the surface Bean-Livingston barrier may occur. What follows then? One may assume that the vortex spiral reaches the cylinder axis and rests there as a straight FL for it seems to present the final stable position for contracting right-handed helix (see Fig. 2). But, as was shown by Clem for a single FL case[1] and then by Brandt for a FLL case,[2] these FL configurations are unstable against the growth of left-handed helical perturbations in the presence of sufficiently large current parallel to the field. This instability, close in nature to spiral instability in magnetohydrodynamics when the conducting fluid is subjected to the longitudinal field, appears due to the destabilizing influence of driving force per unit length $[\mathbf{j}\times\mathbf{\Phi}_0]/c$ exerted by the applied current density upon the FL element. Though the consideration in Refs. 1 and 2 did not account consistently for the influence of the FL interaction with the surface on the FL stability, clearly, this interaction gives rise to instability because of vortex attraction to its image. As will be shown in this section, the account of the surface influence changes the physical picture essentially and, particularly, makes the vortex absolutely unstable (i.e., at zero current) in a certain field range.

To study the stability of the left-handed helix one may use the Gibbs energy expression (33) taken with the upper sign in the last term. The set of curves for various values of current (field) is shown in Fig. 3. The $G(r)$ dependence for unstable vortex (with $\partial G/\partial r<0$) is monoto-

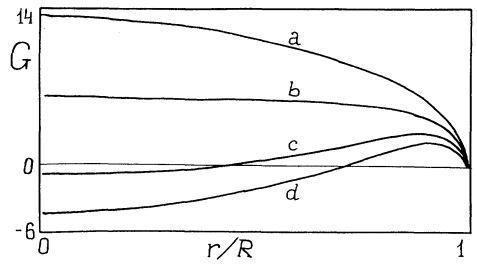


FIG. 3. The Gibbs free energy per unit length [in units of $(\Phi_0/\lambda)^2$] of the SC cylinder of radius $R=0.5\lambda$ containing the left-handed helical magnetic vortex with pitch length $L=0.5\lambda$ vs the helix radius $r$ at $j=0.5j_L$. Various plots correspond to various magnitudes of the applied parallel magnetic field $H/H_C=0$ ($a$), 1 ($b$), 2.6 ($c$), 4 ($d$).

nous, so the study of stability of a straight FL at $r=0$ is sufficient.

Following the notations of Clem's work,[1] we introduce the force exerted upon the unit length of the FL as $f=-\partial G/\partial r=rK(r,L)$. Then, making use of the Gibbs energy approximation for small $r\ll R,L,\lambda$ (see in the Appendix B), one finds

$$K(r,L)=\left[\frac{H_I\Phi_0}{4\pi L\lambda I_1(\kappa_0)}-\frac{H\Phi_0}{8\pi\lambda^2 I_0(\kappa_0)}-\frac{H_{c1}\Phi_0}{4\pi L^2}\left[1+\frac{r^2}{L^2}\right]^{-1/2}\right]$$
$$+\left[\frac{\Phi_0}{4\pi\lambda}\right]^2\left[\frac{1}{\lambda^2}\left[\frac{K_0(\kappa_0)}{I_0(\kappa_0)}+\frac{K_1(\kappa_1)}{I_1(\kappa_1)}\right]+\frac{2}{L^2}\frac{K_0(\kappa_1)}{I_0(\kappa_1)}\right.$$
$$\left.-\frac{1}{L^2}\frac{2I_2(\kappa_1)[K_1(s)/I_1(\kappa_1)+K_0(s)/I_0(\kappa_1)]}{\kappa_1 I_1(\kappa_1)[K_0(s)I_2(\kappa_1)+K_2(s)I_0(\kappa_1)]+2sI_0(\kappa_1)I_2(\kappa_1)K_1(s)}\right]. \tag{39}$$

The unstable modes are defined by the condition $K(0,L)>0$.

The terms in the first large square brackets reproduce the Clem's result obtained without account of the surface influence.[1] In accordance with it, the instability begins when the self-field first attains the critical value

$$H_{Ic}=[2HH_{c1}I_1^2(\kappa_0)/I_0(\kappa_0)]^{1/2}$$

corresponding to critical current $I_c\sim j_L I_1(\kappa_0)/\sqrt{I_0(\kappa_0)}$. The optimal helix pitch length is then $L_0\sim\lambda(2H_{c1}/H_I)I_1(\kappa_0)$. Let us consider separately the cases of thick ($R\gg\lambda$) and thin ($R\ll\lambda$) samples.

### A. $R\gg\lambda$

In this case the $I_c$ value is exponentially large at $\kappa_0=R/\lambda\gg1$ as well as the optimal helix pitch $L_0$. Thus, in the thick sample case the helical instability of a single vortex does not take place. In fact, the instability arises due to forces exerted on the FL by the transport current that is exponentially small deep inside the thick specimen. It is also apparent that the corrections due to the surface influence in the second large square brackets in Eq. (39) do not matter for the same reasons. Moreover, they are as small as $[I_0(\kappa_0)]^{-1}$ even comparing to the terms in the first brackets.

That does not mean, though, that the surface does not affect the flux distribution stability in thick samples. In this case, the problem of FLL stability with respect to helical perturbations should be considered, to say, as was suggested by Brandt,[2] but with a consistent account of the surface influence.

### B. $R<\lambda$

In this case the critical current of instability in Clem's analysis becomes quite meaningful, $j_{ex}\sim j_L(2HH_{c_1}/H_c^2)^{1/2}$. The influence of the surface terms in (39) becomes essential as well. Let us suppose that at low fields an unstable mode has large pitch length $L\gg\lambda$ as well as in the case $R\gg\lambda$. Then $K(0,L)$ acquires the form

$$K(0,L)=\frac{\Phi_0}{8\pi\lambda^2}\left[\left[\frac{\Phi_0}{\pi R^2}-H\right]+\left[\frac{j}{j_L}\right]2H_c y-\frac{\Phi_0}{\pi R^2}y^2\right] \tag{40}$$

for $y\ll1$, where the variable $y=\lambda/L$ is introduced. A drastic difference between this result and that of Clem is that at fields $H<\Phi_0/\pi R^2$ the vortex is absolutely unstable at any currents due to attraction to the surface, since $K(0,L)>0$. That seems quite natural for the presence of a vortex inside the SC cylinder at $H<\Phi_0/\pi R^2$ means that magnetic induction inside the cylinder is higher than outside, which looks unlike the usual SC behavior. Nevertheless, that does not mean the absence of a paramagnetic effect. The time-averaged value of the magnetic moment over the cycle "entry of the right-handed helix, exit of the unstable left-handed helix" may be large.

At the fields $H>\Phi_0/\pi R^2$ the straight FL at $r=0$ is stable at low transport currents. $K(0,L)$ reaches its maximum value,

$$K(0,L)=\frac{\Phi_0}{8\pi\lambda^2}\left[\left[\frac{\Phi_0}{\pi R^2}-H\right]+\frac{\Phi_0}{\pi R^2}\left[\frac{j}{2j_L}\right]^2\frac{R^4}{2\lambda^2\xi^2}\right] \tag{41}$$

for $y_0=(\pi R^2H/\Phi_0-1)^{1/2}$. Thus, in the range of field

$$0<H-\Phi_0/\pi R^2\ll\Phi_0/\pi R^2\sim(\lambda/R)^2H_{c_1}$$

the critical current of helical instability is

$$j_{ex}\cong j_L\frac{2\sqrt{2}\lambda\xi}{R^2}\sqrt{\pi R^2H/\Phi_0-1}\,. \tag{42}$$

If $j>j_{ex}$, $K(0,L)>0$ for all helices with the pitch length in the range $L_-<L<L_+$ around the optimal value $L_0\cong\lambda(\pi R^2H/\Phi_0-1)^{-1/2}\gg\lambda$, where

$$L_\pm=2\sqrt{2}\xi(\lambda/R)^2[j\mp\sqrt{j^2-j_{ex}^2}\,]^{-1/2}j_L^{1/2}\,.$$

When the field $H\gg\Phi_0/\pi R^2$, the assumption $y\ll1$ is no longer valid. Then, in supposition $s\gg1$, one finds the approximation

$$K(0,L)=\frac{\Phi_0}{8\pi\lambda^2}\left[\left[\frac{\Phi_0}{2\pi\lambda^2}\ln\frac{\lambda}{R}-H\right]+\frac{j}{j_L}H_c y-H_{c_1}y^2\right] \tag{43}$$

from which the result close to Clem's one immediately follows:

$$j_{ex}\cong j_L\left[2H_{c_1}\left[H-\frac{\Phi_0}{2\pi\lambda^2}\ln\frac{\lambda}{R}\right]\Big/H_c^2\right]^{1/2}. \tag{44}$$

The first unstable mode is

$$y_0=[(H-\Phi_0\ln(\lambda/R)/2\pi\lambda^2)/2H_{c_1}]^{1/2}\gg 1$$

in accordance with the initial supposition.

## VI. DISCUSSION

In this section, we discuss the possible diagram of the resistive state of a current-carrying superconductor in a longitudinal magnetic field with the account of the above results.

As in this problem we consider the single FL behavior, the results apply directly to the case of a thin specimen with $R<\lambda$. The critical currents for vortex entry and instability are shown in Fig. 4. Since the only characteristic scale for space dependences is $R$, the surface defects of a size $\delta\ll R$ cannot affect essentially the vortex motion and the only characteristic value of the current is the $j_L$, as was emphasized in Ref. 6. $j_L$ is close to the depairing current[16] and is usually much more than the pinning current $j_P$ that allows us to neglect the pinning in a wide range of field.

Since the superconductivity vanishes completely when the transport current $j>j_L$ due to direct pair-breaking process, the resistive state may be realized at lower currents $j<j_L$. In this case, various dissipative regimes may take place depending on the field applied.

Let us consider the increase of the field at some fixed value of measuring current along the upper dashed line on Fig. 4. To the left of point 1 the nondissipative regime takes place, when the FL's cannot enter the specimen. If the sample were cooled in the nonzero field the vortices would be pushed out of it because of their instability. In the region between points 1 and 2 the right-handed helices may enter the sample but, being instable against the left-handed expansion they will leave it immediately. Thus, in this region the oscillating regime of resistivity may occur like that observed on the type-I SC samples.[17,18] Note that though the vortex spiral moves in opposite directions during the two stages of the cycle "entry-exit," the sign of the induced emf is the same because of the change in the sign of the azimuthal component of the field $H_\varphi$ when the right-handed spiral orientation changes into the left-handed one (compare with results of Ref. 1). To the right of point 2 the vortex enters the sample and rests there preventing an extra vortex from entry into the cylinder. Thus, while increasing the field, in this region the reentrant nondissipative state may appear and exist up to the highest fields of the order of $H_{c_2}$. Though the vortex rested at the axis of the cylinder cannot prevent the entry of the vortex rings at sufficiently large currents and, in principle, the dissipative scenario may be realized like that in the absence of field as was discussed in Refs. 4–6 and 19. Note that the dissipation processes due to helix and ring entry are quite different. Really, when the helical vortex enters the specimen the coherent voltage signal from different flights of the spiral may induce quite a large single-voltage impulse or periodical oscillations. On the contrary, the stochastic incoherent entry of the vortex rings may induce only a white voltage noise without any characteristic frequencies as was discussed in Ref. 20.

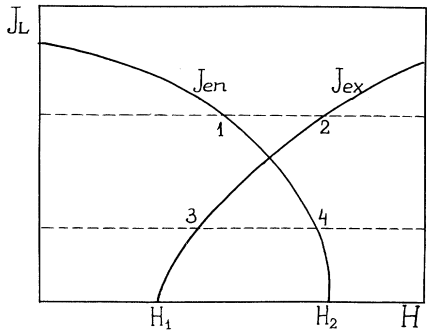


FIG. 4. The sketch of the possible diagram of the resistive state of the SC cylinder in a parallel magnetic field in the current-field coordinates $j$-$h$ discussed in detail in Sec. VI. The plots describe the critical currents of right-handed helix entry and left-handed helix exit. The characteristic fields $H_1=\Phi_0/\pi R^2$ and $H_2\cong(2\lambda/R)H_C$.

Let us emphasize that in the region to the right of point 2 the nonzero time-averaged paramagnetic moment may be observed with the induction $B\le H+\Phi_z(0)/\pi R^2$, where $\Phi_z(0)$ is taken from Eq. (18).

When measuring at lower transport currents (the lower dashed line in Fig. 4) the nondissipative state may take place in the region to the left of point 4. In the region between points 3 and 4 the permanent magnetic moment determined by the equation $M=\Phi_z(0)/4\pi^2R^2$ may be realized, if the specimen is cooled in the field. The zero-field-cooled specimen should not exhibit the magnetic moment in this region. While increasing the field to the right of point 4, the vortex may enter and be stable inside the sample. Then the nondissipative state may take place up to the highest field of order of $H_{c_2}$. Thus, at small measuring currents the oscillating regime of dissipation cannot take place.

In the case of the thick samples with $R\gg\lambda$ the picture becomes much more complicated. A sharp dependence of the surface barrier width on the current and field[6] provides that at the currents $j>j_{c_1}\cong j_L/\kappa\ll j_L$ ($\kappa=\lambda/\xi$ is the Ginzburg-Landau parameter) the entry of FL fragments becomes possible on the surface defects of the size of $\lambda$. The pinning also may essentially affect the vortex motion when $j_p\sim j_{c_1}$. Though, the critical current of single-vortex instability is exponentially large, the critical current of a helical instability of the FLL may be rather small and even equal to zero, as was stated by Brandt.[2]

Also, in addition to the barrier and instability reasons considered here, other and more subtle mechanisms of resistivity may be realized[21] in type-II SC's. Anyway, the variety of resistive regimes may take place, since the pinning may prohibit either contracting or expanding vortices. Particularly, if the $j_{ex}, j_p < j_{c_1} < j \ll j_L$ the oscillating regime of dissipation may arise.

It would be also interesting to study the samples of intermediate size of some $\lambda$'s which permit the entry of a few vortices but are characterized by not so large critical current of single-vortex instability. In such a case the dissipative cycle conditioned by the oscillation of a pair of helical vortices of different vorticity may arise, as was suggested by Clem.[1]

## VII. CONCLUSIONS

A problem of a helical magnetic vortex in a current-carrying superconducting cylinder subjected to a longitudinal magnetic field was solved exactly in the London approximation. Gibbs free energy of the superconducting cylinder containing the vortex was calculated with regard to the work done by the sources of the constant transport current and external magnetic field. It allowed us to evaluate a critical current and field of the spontaneous entry of right-handed helical flux line into the sample against the surface Bean-Livingston barrier, using the criterion of the barrier vanishing. An optimal helix was found for which the barrier was the least and which, hence, was the first to enter the sample. In the thick sample case (with radius $R \gg \lambda$) this helix turned out to follow the pattern of the full magnetic field on the surface including the external field and transport current self-field. In this case, the breakdown of the nondissipative state was shown to occur when the full field at the surface first attained the magnitude of the thermodynamical critical field $H_c$. The latter statement extends the validity of Silsbee's rule[14] to the case of the longitudinal magnetic field applied to the specimen.

The obtained Gibbs free energy enabled us to also calculate the critical current of instability of a linear vortex lying on the cylinder axis with respect to the left-handed helical distortions that was first considered by Clem.[1] Being, in principle, the same for the case of thick sample our results turned out to be quite different in the thin sample case, $R < \lambda$, where the absolute instability of the vortex was established.

Based on the above results the diagram of the resistive state of the current-carrying superconductor subjected to a parallel magnetic field was evaluated and the possible influence of the surface defects and pinning was discussed. The variety of the resistive regimes might be expected depending on the field and current values, pinning strength, and quality of the surface, particularly the regime with oscillating dissipation, like that observed in experiments on the type-I superconductors.[17,18] In the latter case the value of the paramagnetic effect was estimated.

## ACKNOWLEDGMENTS

I would like to thank Professor Yu. V. Medvedev for permanent attention towards and support of this work and Dr. Yu. E. Kuzovlev for helpful remarks on the boundary-condition problem. Valuable discussions with Professor J. R. Clem, Dr. E. H. Brandt, Dr. A. Yu. Martynovich, Professor H. C. Freyhardt, Professor V. M. Pan, Professor L. M. Fisher, and Professor A. M. Campbell are gratefully acknowledged. I am grateful to German State Foundation DAAD and Metal Physics Institute of Goettingen University for hospitality during the research visit to Goettingen where this work was completed.

## APPENDIX A

In the simplest linear[9] or ring[6] FL configurations the vortex-induced magnetic field vanishes at the sample surface. In contrast to this, helical FL creates the nonzero field at the surface and in the outer space. Here we evaluate the free energy correction following from this fact.

Let us transform expression (21) making use of the vector identity following it

$$F=\frac{1}{8\pi}\int_{\rho\le R}\mathbf{h}(\mathbf{h}+\lambda^2\mathrm{curlcurl}\mathbf{h})dV + \frac{1}{8\pi}\int_{\rho\le R}\lambda^2\mathrm{div}[\mathbf{h}\times\mathrm{curl}\mathbf{h}]dV + \frac{1}{8\pi}\int_{\rho\ge R}(\bar{v}\psi)^2 dV \,. \tag{A1}$$

First integral in (A1) transforms to formula (22) due to Eq. (1). The rest of the RHS of (A1) forms the energy correction that reads

$$\Delta F=\frac{R}{16\pi^2 L}\int_{-\pi}^{\pi}d\varphi\int_{-\pi L}^{\pi L}dz\left\{\lambda^2\left[\frac{1}{\rho}h_\varphi^2+h_\varphi\frac{\partial h_\varphi}{\partial\rho}-\frac{1}{\rho}h_\varphi\frac{\partial h_\rho}{\partial\varphi}-h_z\frac{\partial h_\rho}{\partial z}-h_z\frac{\partial h_z}{\partial\rho}\right]-\psi\frac{\partial\psi}{\partial\rho}\right\}. \tag{A2}$$

Making use of Fourier representation of field components [see after formula (6)] we transform (A2) to

$$\Delta F=\frac{R}{\pi L}\sum_k\left\{\lambda^2\left[b_k\left[\frac{b_{-k}-ika_{-k}}{R}+b'_{-k}\right]+\frac{ikc_k a_{-k}}{L}+c_k c'_{-k}\right]-\psi_k\psi'_{-k}\right\}. \tag{A3}$$

The expression for the derivative $b_k'$ may be found thanks to Maxwell Eq. (16) and Eq. (7)

$$b_k'=-\frac{b_k}{R}+\frac{R}{L}c_k'+\frac{a_k}{ikR}(k^2+\kappa_k^2)\ . \tag{A4}$$

Then upon substitution of Eq. (A4) and boundary conditions (11) into Eq. (A3) one finds

$$\Delta F=0\ .$$

This result is in contrast to that of Ref. 11 obtained for type-I SC's where the contribution to the free energy of the field outside the sample is responsible for the unusual field dependence of critical current.

## APPENDIX B: FREE-ENERGY CALCULATION

In a wide range of radius values $r<R$, except $r\ll R,L,\lambda$, the corrections following from $d_k$ terms in Eqs. (12), (13), and (15) are small as $s^2$ at $s\ll 1$ and as $\exp[-2s(1-r/R)]$ at $s\gg 1$, where $s=R/L$. Omitting $d_k$ in expressions (12), (13), and (15) one can carry out the summation in formulas

$$\eta_\varphi(r,0)=b_0+2\sum_{k=1}^{\infty}b_k(r-\xi)\ ,$$
$$\eta_z(r,0)=c_0+\sum_{k=1}^{\infty}c_k(r-\xi)\ , \tag{B1}$$

taking into account the slow convergence of these series. The latter allows us to use for the modified Bessel functions the asymptotic representation[8]

$$I_k(\kappa_k x)=\frac{\exp[k\varphi(xs)]}{\sqrt{2\pi k}\,(1+x^2s^2)^{1/4}}$$

and

$$K_k(\kappa_k,x)=\frac{\exp[-k\varphi(xs)]\sqrt{\pi}}{\sqrt{2k}\,(1+x^2s^2)^{1/4}}\ ,$$

where $\varphi(s)=(1+s^2)^{1/2}-\ln[1/s+(1+1/s^2)^{1/2}]$. The values $\kappa_0=R/\lambda$ and $\kappa_k\cong ks$ at $k\gg L/\lambda$ were used above. Then the free energy $F$ reads

$$F=\left[\frac{\Phi_0}{4\pi\lambda}\right]^2\left\{P_0^0(r,r)+\frac{r^2}{L^2}P_1^0(r,r)+\sqrt{1+r^2/L^2}\ln\left[\frac{1-\exp\{2[\varphi(r/L)-\varphi(R/L)]\}}{(\xi/L)[L/r+(r/L)(1+\sqrt{1+r^2/L^2})^{-1}]}\right]\right\} \tag{B2}$$

from which expression (23) follows.

In the case $r\ll R,L,\lambda$, the corrections from $d_k$ are no longer small. Though it appears that the terms with $k>2$ in sums (B1) are as small as $(r/\lambda)^{2k}$, $(r/L)^{2k}$, or $(r/R)^{2k}$. Then, restricting ourselves in sums (B1) to the terms with $k=0,1$, we find

$$F=\left[\frac{\Phi_0}{4\pi\lambda}\right]^2\left\{\sqrt{1+r^2/L^2}\ln\frac{\lambda}{\xi}-\frac{K_0(\kappa_0)}{I_0(\kappa_0)}-\frac{r^2}{2\lambda^2}\left[\frac{K_0(\kappa_0)}{I_0(\kappa_0)}+\frac{K_1(\kappa_1)}{I_1(\kappa_1)}\right]-\frac{r^2}{L^2}\frac{K_0(\kappa_1)}{I_0(\kappa_1)}\right.$$
$$\left.+\frac{r^2}{L^2}\frac{I_2(\kappa_1)[K_1(s)/I_1(\kappa_1)+K_0(s)/I_0(\kappa_1)]}{\kappa_1 I_1(\kappa_1)[K_0(s)I_2(\kappa_1)+K_2(s)I_0(\kappa_1)]+2sI_0(\kappa_1)I_2(\kappa_1)K_1(s)}\right\}. \tag{B3}$$


[1] J. R. Clem, Phys. Rev. Lett. **38**, 1425 (1977).

[2] E. H. Brandt, Phys. Lett. **A79**, 207 (1980); Phys. Rev. B **25**, 5756 (1982).

[3] R. P. Feynmann, *Progress in Low Temperature Physics* (North-Holland, Amsterdam, 1964), Vol. 1, pp. 17–53.

[4] A. M. Campbell and J. E. Evetts, *Critical Currents in Superconductors* (Taylor & Francis, London, 1972).

[5] I. M. Gordion, Sverkhprovodimost (Moscow) **5**, 1701 (1992).

[6] Yu. A. Genenko, Phys. Rev. B **49**, 6950 (1994).

[7] One can easily make sure that the field continuity provides that normal current component $j_n=0$ at the sample surface. Note that the latter requirement results in zero boundary condition in a vortex ring problem (Ref. 6). In the spiral vortex case, though, there is no continuous solution of Eqs. (1) with zero field on the surface.

[8] *Handbook of Mathematical Functions*, edited by M. Abramovitz and I. Stegun, Appl. Math. Ser. No. 55 (U.S. GPO, Washington, D.C., 1965).

[9] L. L. Daemen and J. E. Gubernatis, Phys. Rev. B **43**, 413 (1991).

[10] V. A. Kozlov and A. V. Samokhvalov, Pisma Zh. Eksp. Teor. Fiz. **53**, 150 (1991) [JETP Lett. **53**, 158 (1991)].

[11] J. R. Clem, R. P. Huebener, and D. E. Gallus, J. Low Temp. Phys. **12**, 449 (1973).

[12] M. Tinkham, *Introduction to Superconductivity* (McGraw-Hill, New York, 1975).

[13] V. V. Chmidt, *Introduction to Physics of Superconductors* (Nauka, Moscow, 1982).

[14] F. B. Silsbee, J. Wash. Acad. Sci. **6**, 597 (1916).

[15] H. Jiang, Y. Huang, H. How, S. Zhang, C. Vittoria, A. Widow, D. B. Chrisey, J. S. Horwitz, and R. Lee, Phys. Rev. Lett. **66**, 1785 (1991).

[16] J. Bardeen, Rev. Mod. Phys. **34**, 667 (1962).

[17] T. S. Teasdale and H. E. Rorschax, Phys. Rev. **90**, 709 (1953).

[18] I. L. Landau, Zh. Eksp. Teor. Fiz. **64**, 557 (1973) [Sov. Phys. JETP **37**, 285 (1973)].

[19] Yu. A. Genenko, Physica C **215**, 343 (1993).

[20] H. L. Watson and R. P. Huebener, Phys. Rev. B **10**, 4577 (1974).

[21] D. S. Fisher, M. P. A. Fischer, and D. A. Huze, Phys. Rev. B **43**, 130 (1991).